

ZnO:Al films deposited by in-line reactive AC magnetron sputtering for a-Si:H thin film solar cells

V. Sittinger<sup>1,\*</sup>, F. Ruske<sup>1</sup>, W. Werner<sup>1</sup>, B. Szyszka<sup>1</sup>, B. Rech<sup>2</sup>, J. Hüpkes<sup>2</sup>, G. Schöpe<sup>2</sup>, H. Stiebig<sup>2</sup>

<sup>1</sup>Fraunhofer Institute for Surface Engineering and Thin Films IST, Bienroder Weg 54e, 38108 Braunschweig, Germany

<sup>2</sup>Institute of Photovoltaics IPV, FZ-Jülich, D-52425 Jülich, Germany

Abstract

Throughout the last years strong efforts have been made to use Al-doped ZnO films on glass as substrates for amorphous or amorphous/microcrystalline silicon solar cells. The material promises better performance at low cost especially because ZnO:Al can be roughened in order to enhance the light scattering into the cell. Best optical and electrical properties are usually achieved by RF sputtering of ceramic targets. For this process deposition rates are low and the costs are comparatively high. Reactive sputtering from metallic Zn/Al compound targets offers higher rates and a comparable high film quality in respect to transmission and conductivity. In the presented work the process has been optimised to lead to high quality films as shown by reproducible cell efficiencies of around 9 % initial for single junction amorphous silicon solar cells on commercial glass substrates. The crucial point for achieving high efficiencies is to know the dependency of the surface structure after the roughening step, which is usually performed in a wet etch, on the deposition parameters like oxygen partial pressure, Al-content of the targets and temperature. The most important insights are discussed and the process of optimisation is presented.

**Keywords:** Aluminium doped zinc oxide films, solar cells, sputter deposition

1. Introduction

Within the scope of an increased importance of renewable energy sources photovoltaics has experienced an increased scientific and economic interest. Solar cells based on silicon wafer technology are being produced in large amounts and account for over 90 % percent of the solar cell market [1].

In expectation of technological progress it is commonly accepted that the costs for solar energy will be dominated by the silicon material cost. The so-called second generation solar cells therefore make use of thin film active layers where light conversion takes place in layers only a few microns thick. Thin film solar cells based on amorphous or microcrystalline silicon (a-Si:H,  $\mu\text{c-Si:H}$ ) are examples for this type of solar cell. A good overview on the potential of this cell type can be found in [2], more aspects are found in [3].

High quality solar cells strongly rely on the quality of transparent and conductive oxide (TCO) films used as front contacts. This is especially true for superstrate (Fig. 1) cells where the solar cell is deposited top to bottom onto a glass substrate.

The requirements which these films have to meet are numerous: (a) light loss in the front layers has to be prevented by minimisation of optical absorption, (b) the resistivity has to be as low as possible in order to keep the required film thickness for a good current transport small (lower deposition time, lower cost, less optical losses) and (c) the material cost has to be low.

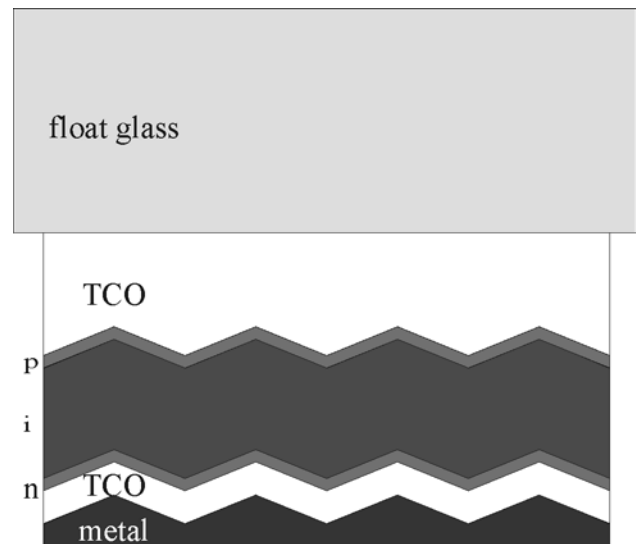


Fig 1. Layer structure of a p-i-n- (superstrate) solar cell.

The minimisation of optical losses implies a matching of optical properties of the TCO material to the absorbing layer. While low optical absorption in the visible range is a common optimisation goal for all researchers of TCO films the transmission window has to be extended to the band gap of the absorbing layer in the case of solar cells. For a-Si:H with a bandgap of around 1.7 eV and  $\mu\text{c-Si:H}$  (1.1 eV) this means that the plasma wavelength has to be increased to values of 750 and 1150 nm, respectively. According to Drude's theory the optical properties in the near infrared (NIR) are closely linked to the properties of

free carriers in the material and the plasma wavelength is proportional to the square root of the free carrier concentration:

$$\omega_p = \sqrt{\frac{4\pi \cdot n_e e^2}{m^*}} \quad (1)$$

where  $\omega_p$  stands for the plasma frequency,  $n_e$  denotes the concentration of free carriers and  $e$  and  $m^*$  stand for the elemental charge and the effective electron mass, respectively. This means the carrier concentration in the films has to be reduced. The film resistivity  $\rho$  also depends on the carrier concentration:

$$\rho = \frac{1}{\mu \cdot n_e \cdot e} \quad (2)$$

where  $\mu$  is the electron mobility. As low resistivity is required and carrier concentration is limited by Eq. (1), high electron mobilities have to be reached.

One additional aspect of a-Si:H, but even more for  $\mu$ -Si:H, cells is the low absorption in the NIR region. Usually only a small part of the light is converted to current for long wavelengths upon a single pass through the absorbing layer. Therefore an efficiency increase can be achieved if the light is confined in the cell by multiple reflections at back and front side (light trapping). This confinement can be reached by an adequate light scattering at the TCO/absorber interface which can be caused by a rough TCO surface [4].

In practice fluorine doped tin oxide (SnO:F) films are used as TCO films. They can be produced in a cheap way by thermal CVD if the glass is coated right at the float line [5].

An alternative with high potential are aluminium doped zinc oxide (ZnO:Al or AZO) films, which can also be produced on large scale by magnetron sputtering and allow for good light scattering after the surface has been roughened up by a wet chemical etching process [6 and references therein]. In this paper the optimisation of a reactive magnetron sputtering process to the needs of state-of-the-art thin film silicon solar cells is discussed. While the process itself has been described in detail elsewhere [7-9], the upscaling of the process and the adaptation to the requirements described above are explained in detail. Parts of the work have already been published [10-13].

## 2. Experiment

The films discussed in this paper were deposited using the vertical in-line sputtering system Leybold A700V [8], equipped with a pair of rectangular magnetrons driven by an Advanced Energy PEII MF power supply at 40 kHz. The usual configuration was a Leybold TwinMag<sup>TM</sup> sputtering source consisting of two PK 750 cathodes while an alternative setup with moving magnets (CleanMag<sup>TM</sup>) [10, 14] has also been tested. As transparent and conductive ZnO:Al films are only

obtained in the unstable transition region of the reactive process, a control loop system was implemented that monitors the state of the discharge by measuring oxygen partial pressure with a  $\lambda$ -sensor. The discharge power is then adjusted accordingly in order to keep the oxygen partial pressure at the desired level.

Optical properties were determined by measuring transmission and reflection in the spectral range from 250 to 2500 nm using a double beam spectrophotometer (Varian Cary-5) and by spectroscopic ellipsometry at variable angle (SEVA) from 250 to 850 nm using a Sentech SE 850. Sheet resistance was determined with a four point probe. Further evaluations were focussed on the applicability in a-Si:H solar cells. First, the etching behaviour was tested and the resulting surface morphology was observed by scanning electron microscopy (SEM). Subsequently, a-Si:H solar cells were deposited onto selected substrates and characterised with respect to their initial J-V characteristics and in particular regarding the current density under red light illumination.

## 3. Initial situation

TCO films with high transparency and low resistivity were obtained at substrate temperatures between 150 and 200 °C [8, 10] during deposition. Lower substrate temperatures usually resulted in increased optical absorption while Zn desorption from the growing film was observed for higher temperatures, leading to inferior electrical properties. In this temperature window deposition series with varying total pressure were carried out, and oxygen partial pressure was varied in order to reach lowest possible resistivity for high-transparent films. Usually, low resistivity is reached in an oxygen partial pressure window of only a few mPa [10, 11], with strongly absorbing layers for lower oxygen partial pressures and highly resistive films for high oxygen partial pressures. The samples were etched and the result visually examined, as increased light scattering (high haze) can already be detected by looking at the sample. The samples chosen for deposition of solar cells were deposited at the highest oxygen partial pressure still leading to low resistivities, since these samples showed the highest haze. The TCO properties and results obtained for a-Si:H cells are summarised in table 1 (see also Fig. 2 in [11]). The resistivity of the films used for deposition of solar cells differed from values published, since substrates were not taken from a central position of the carrier and inhomogenities can be large [9]. The surface after etching was also inspected by SEM, the pictures are shown in Fig. 2. The difference is obvious, with sample A showing a rather smooth surface while sharp spikes are observed on sample C. This leads to increased light scattering and hence an increased light scattering that can be nicely observed in the red light current density  $j_{sc}(\text{red})$  [11]. The reason for the different etching behaviour is not evident, as it is known to depend on many parameters like oxygen amount in front of the sample during deposition,

the total pressure, the substrate, substrate condition, deposition temperature and etching time.

**Table 1.** TCO deposition conditions, properties and results obtained for a-Si:H cells.

		sample A	sample C
System parameters	$p_{tot}$ (mPa)	130	970
	$T_s$ (°C)	200	200
	$p_{O_2}$ (mPa)	31	42
Film parameters	$d$ (nm)	948	957
	$\rho$ ( $\mu\Omega\text{cm}$ )	592	417
	$k$ (550 nm)	$3.3 \cdot 10^{-3}$	$4.0 \cdot 10^{-3}$
Cell parameters	$\eta_{iii}$	8.07	9.37
	$J_{sc}$ ( $\text{mA}/\text{cm}^2$ )	13.60	15.84
	$J_{sc}$ (red) ( $\text{mA}/\text{cm}^2$ )	4.27	5.56
	FF (%)	68.2	70.0

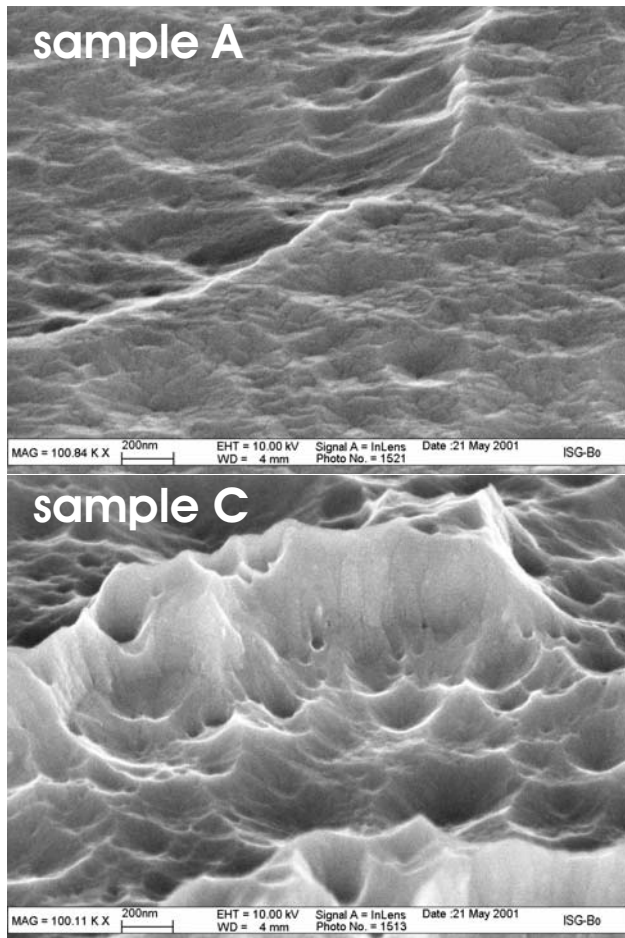


**Fig. 2.** SEM images of two etched ZnO:Al films for low (sample A) and high sputter pressure (sample C) after etching in 0.5% HCl removing 150 nm of film thickness.

Extrapolation of one of these parameters is virtually impossible for several reasons. First, the etching time has to be normalised to etching rate and surface structure can vary drastically with etching time. Second, the substrate condition is not easily controllable. For example even after cleaning marks left by spacers used during transport can influence the etching process. Finally the etching behaviour shows a strong dependency on working point [15], in our case oxygen partial pressure, which has to be compared to the observed S-curves in reactive magnetron sputtering which vary with substrate temperature, total pressure, gas flow rate, pumping rate and target condition [16].

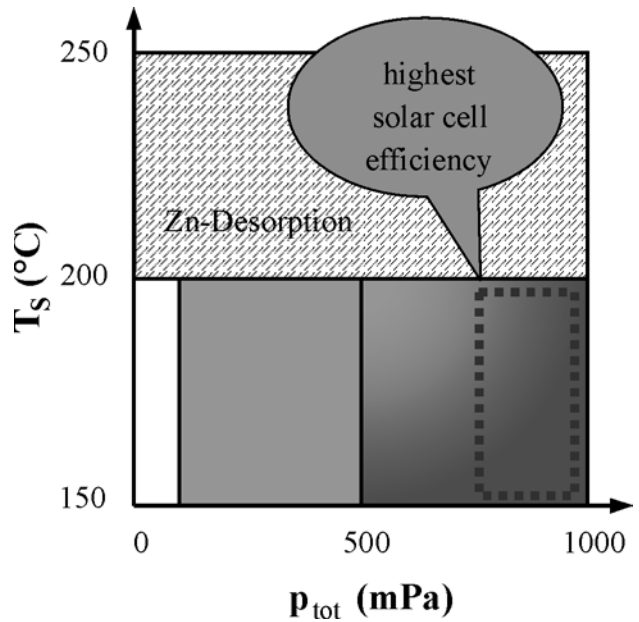


**Fig. 3.** Preferred deposition conditions for a stable process are temperatures below 200 °C and deposition pressures lower than 500 mPa. The best a-Si:H cell efficiencies are obtained for total pressures higher than 800 mPa where the deposition process of AZO tends to be unstable.

The conclusion drawn in [11] and [12] was to deposit films at high pressure and moderate temperatures between 150 and 200 °C. Fig. 3 shows the preferred deposition conditions and the limitations. As indicated in the lower right part increasing pressure leads to increasing instability of the deposition process. The TCO material properties depend strongly on working point and in order to obtain good results a stable process throughout the whole deposition time is required. In practice this gets increasingly difficult for large areas, since the working point may drift for different positions on the targets. In extreme situations the target can run in severe different conditions at its ends [17]. In order to yield homogenous film properties with respect to target axis, a symmetry control has been implemented [18]. A second issue concerning the implementation of a production process is

reproducibility. Fig. 4 shows cell results obtained from 2001 to 2003.

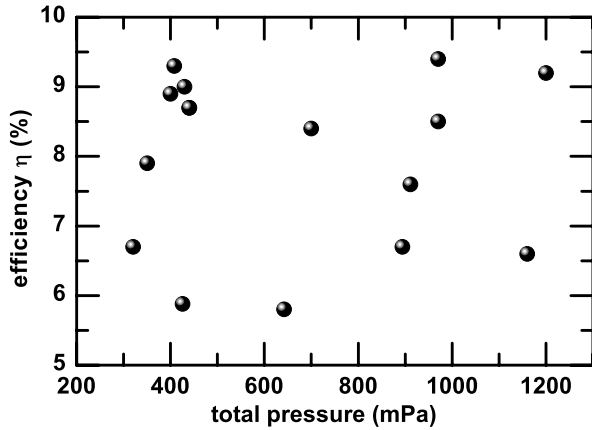


Fig. 4. Non reproducibility of initial efficiencies of a-Si:H solar cells deposited at different total deposition pressures.

As can be seen the efficiencies scatter drastically and to repeat deposition conditions like total pressure and substrate temperature is not sufficient to obtain comparable results, even on the same coater. It was found out that one of the most important reasons for these problems are the float glass substrates, where the coating side has a strong influence [19] and cleaning has to be optimised. Also different types of glass not only have a different surface chemistry but also show a different behaviour in respect to heating in the coater due to different emissivities. It was found that the use of a SiO<sub>2</sub> interface layer on the glass substrate prior to TCO deposition can improve the situation and suppress glass surface effects to a large extend if the larger particles are removed by a suitable cleaning procedure.

## 4. Recent developments

### 4.1 Moving magnets

As cost is one of the most important goals for the TCO an effort was made to increase target utilisation. While the most popular solution for the problem are rotatables it is also possible to move the magnets behind a planar target. One system using this technique is the CleanMag™ which was tested on the A700V coater. All depositions were carried out at 500 mPa, while oxygen partial pressure was varied and optimised for substrate temperatures between room temperature and 250 °C. In order to prevent problems with aluminium segregation at high temperatures, a target concentration of 1 wt.% has been chosen instead of the 2 wt.% used before. Since the experiments were all carried out using the same target inferior properties were expected for low substrate temperatures.

Fig. 5 shows the resistivities obtained for temperatures between 50 and 250 °C.

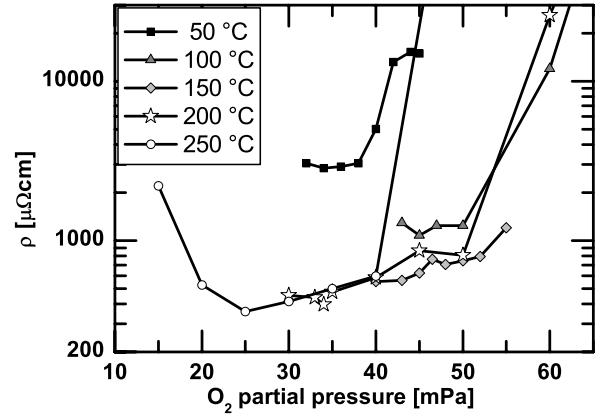
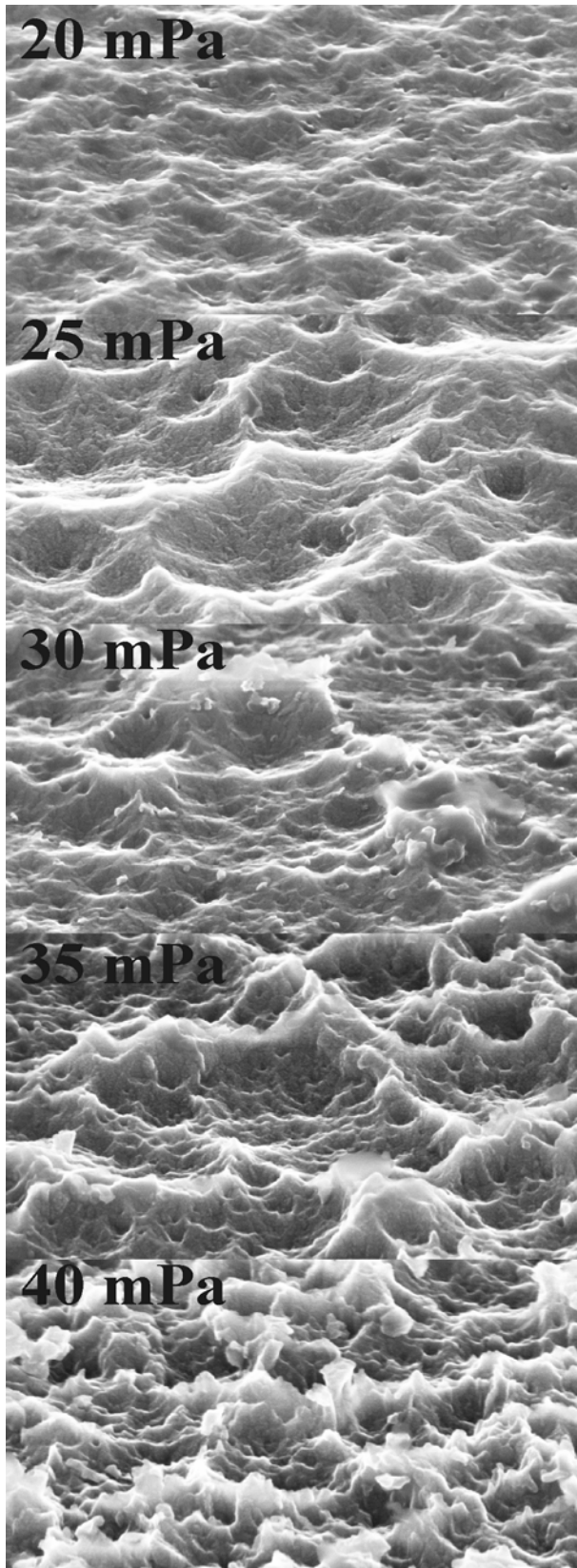
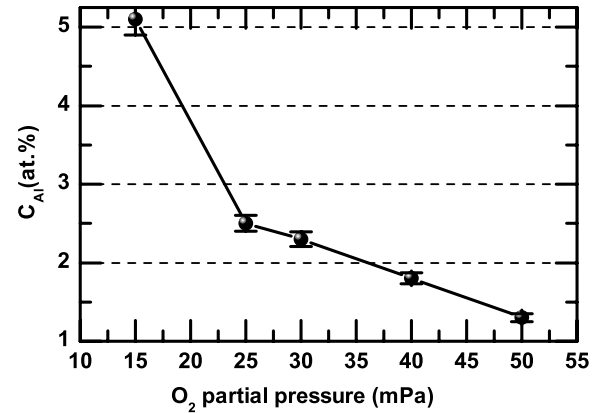


Fig. 5. Dependence of resistivity of AZO films deposited with the CleanMag™ cathode on oxygen partial pressure for different substrate temperatures.

The resistivity minimum obtained by varying the oxygen partial pressure decreases with increasing substrate temperature and resistivities below 400  $\mu\Omega\text{cm}$  were obtained at 250 °C, the highest temperature studied. Optical absorption, including absorption in the substrate, was below 4% for all films deposited at 250 °C. For lower temperatures the optical properties were inferior, with most samples deposited at lower oxygen partial pressures showing unacceptable absorption. The effect is well known and absorption is usually attributed to a slight sub-stoichiometry of the ZnO. For this reason the feasible process window gets very small when the substrate temperature is lowered. Fig. 6 shows the etching behaviour of the samples deposited at 250 °C, with increasing oxygen partial pressure from top to bottom. The behaviour observed coincides well with the results obtained by Hüpkes et al. [15]. For low oxygen partial pressures, thus operating points close to the metallic mode, the resulting surface structures appear rather smooth and the samples show only weak light scattering when observed visually. In contrast to this films deposited at higher oxygen partial pressures towards the oxide mode display very rough surfaces with sharp structures distributed over the surface. It is also observed that the average size of the observed structures decreases. The light scattering on the rough samples is also very clear by visual inspection. It is interesting to note, that the aluminium content of the samples, as determined by electron probe micro analysis (EPMA), changes strongly (Fig. 7). While the highest oxygen partial pressure leads to an aluminium concentration close to the 1.2 at.% expected from the target concentration, values of over 5 at.% are observed for operating points close to metallic mode. It is assumed this will have a strong effect on the etching behaviour. Unfortunately films were too thin (0.5  $\mu\text{m}$ ) to deposit high quality solar cells and only two test cells indicating the high potential of the films could be deposited.



**Fig. 6.** SEM images of ZnO:Al films deposited under different oxygen partial pressures after 150 nm were removed from the total thickness by etching in 0.5% HCl.



**Fig. 7.** Influence of the oxygen partial pressure on the Al content of AZO films deposited with the CleanMag™ cathode.

#### 4.2 Insights from reactive sputtering at IPV

As described before, AZO deposition at IST was focussed on deposition temperatures below 200 °C. Deposition conditions were optimised with respect to transparency and conductivity.

In a new coater at IPV a different approach was taken and the low deposition temperature, favourable for most alternative applications of AZO like CIS-based solar cells or TCO on plastic foils, were dropped in favour of a process optimized for high optical transmission in the NIR spectral region and an etching behaviour suited for reaching efficient light trapping.

For this reason aluminium concentration in the target was decreased further to 0.5 wt.% or less and depositions were carried out at substrate temperatures of up to 300 °C [15, 20, 21]. At these process conditions the films obtained rarely show optical absorption as excess zinc is usually evaporated from the surface of the growing film and high Hall mobilities can be observed. The reason for high mobilities is the reduced carrier concentration, resulting in lower carrier scattering by ionised impurities, and a low defect density that also helps the etching behaviour, since a fast etching attack down to the substrate, leading to holes in the TCO layer, is suppressed. A second new approach was taken by passing the substrate multiple times in front of the target. This led to an improved and more predictable etching behaviour since inhomogeneities usually obtained in static deposition are better cancelled out for fast substrate movement in multiple passes than in a single pass with slow speed [22]. Summarised the changed deposition conditions led to a process that is easier to reproduce and resulting AZO layers have a suitability for a-Si:H solar cells close to that of RF sputtered AZO films [23].

### 4.3 High temperature deposition

As the approach of using lower deposition temperatures showed poor reproducibility, new deposition series at increased substrate temperatures were carried out with two different target concentrations of 1 and 2 wt.% aluminium. Samples were deposited at a total pressure of 400 and 900 mPa at each temperature and oxygen partial pressure was varied in order to achieve optimal cell performance. The conditions are summarised in table 2.

**Table 2.** Deposition conditions for presented samples

Process	Reactive MF magnetron sputtering Leybold PK 750 TwinMag™ cathode excited at 40 kHz, Advanced Energy PEII	
System parameters	Distance target-substrate	$d_{ST}$ 90 mm
	Target material	Zn: 1 wt% Al Zn: 2 wt% Al
	Gas flow	$q_{Ar}$ 2 x 100 sccm $q_{O_2}$ 15 – 45 sccm
Process parameters	Substrate temperature	$T_S$ 180 °C, 200 °C, 220 °C, 240 °C, 260 °C
	Discharge power	P ~ 3000...6000 W
	Total pressure	$p_{tot}$ 400 mPa, 900 mPa
	Substrate	Saint Gobain Diamond Corning glass
	Substrate size	10 x 10 cm <sup>2</sup>
	Film thickness	d 600 ... 1000 nm

The best resistivities reached for both targets and the corresponding optical absorption are shown in Fig. 8, not regarding the type of substrate they were deposited onto. The necessity to go to lower aluminium contents in the target when depositing films at higher temperatures is evident. The target with 2 wt.% shows a constant increase of the lowest resistivity reached with increasing temperature. For lower aluminium concentrations the temperature can be increased further and lower resistivities are achieved. Optical absorption of the corresponding samples is reduced with increasing substrate temperature.

It is important to mentioned that the values do not reflect the lowest absorption observed in the series. The main conclusion that can be drawn from the absorption in Fig. 8 is, that it is easier to reach low resistivity and low absorption simultaneously at higher temperatures.

The aluminium concentration in the film can be different from the target. Assuming a perfect  $Zn_{1-x}Al_xO$  stoichiometry we expect an aluminium concentration of 2.4 and 1.2 at.% in the film for the 2 wt.% and the 1 wt.% target, respectively.

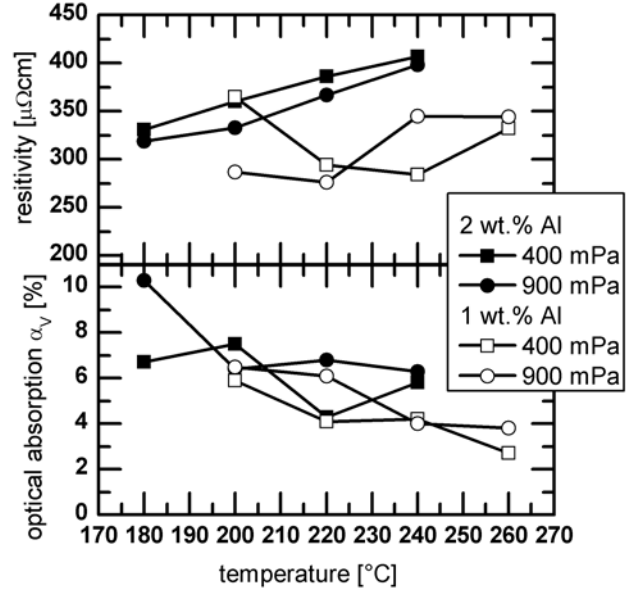


**Fig. 8.** Dependence of resistivity and optical absorption on deposition temperature of the substrate for different chamber pressure and Al content.

The aluminium content actually determined in the film by EPMA is shown in Fig. 9 for the films deposited at 400 mPa total pressure with the 1 wt.% target. It is observed that all samples show a much higher aluminium content than expected. It can also be seen that the aluminium content diminishes with increasing oxygen partial pressure and usually the content is increased by higher temperatures. This effect is caused by the evaporation of metallic zinc from the growing film surface and can be explained if we assume that aluminium and oxidised zinc do not desorb from the substrate in the temperature range used in these coatings.

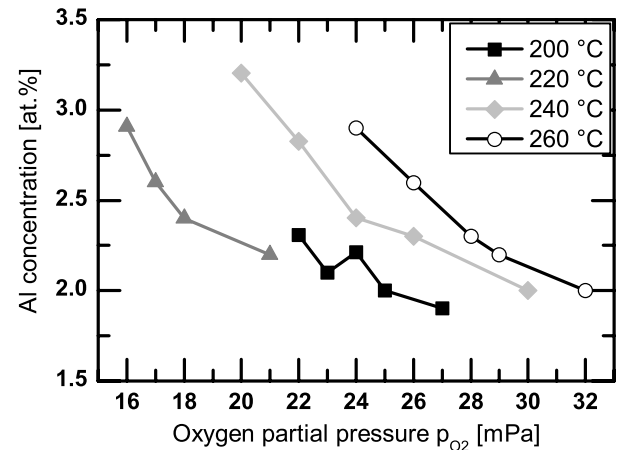


**Fig. 9.** Influence of the oxygen partial pressure on the Al content of AZO films deposited at different substrate temperature.

Since the oxide fraction at the substrate ( $\theta_s$ , for definition see [16]) rises with increasing oxygen partial pressure less

metallic zinc will evaporate from the surface and the zinc-to-aluminium-ratio will not increase as much as for lower partial pressures.

The desorption effect is even increased for increasing substrate temperature as desorption is an energy-driven process. This is also a possible explanation for lower optical absorption with increasing deposition temperature (Fig. 8). A precise application of Berg's model to the experiments described here in order to compare predictions of deposition rates and substrate oxide fraction to the observations made is planned.

Etching was performed on all samples and etching times varied so that 150 nm were removed from each sample. The general behaviour is similar to the case of the samples deposited by CleanMag™ (Fig. 6) and at IPV [15]: the samples remain rather flat and show large structures for deposition carried out at low partial pressures and get rougher with smaller features as the working point is shifted towards oxide mode. Some samples showed spots where holes down to the substrate are etched into the sample (Fig. 10).

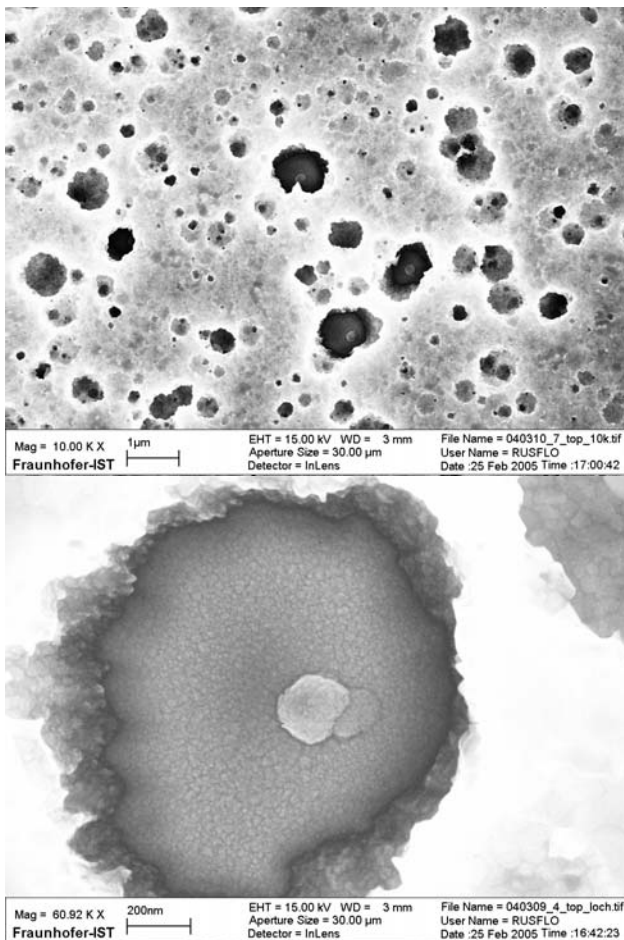


**Fig. 10.** SEM images of after etching in 0.5% HCl removing 150 nm of film thickness. Inside the holes are particles. This is a serious problem for solar cells as too steep structures can shunt the cell and significantly diminish

performance. With increased magnification under the SEM it was observed, that the vast majority of holes was caused by particles underneath the AZO layer (Fig. 10, bottom). It is believed that these particles cause pinholes that show dramatically increased etching rates. Solar a-Si:H cells were deposited on chosen substrates that showed good light scattering by visual inspection and a low sufficiently sheet resistance after etching. This normally implies low hole density as increased hole formation during etching usually results in high sheet resistances. The initial efficiencies for the target with high aluminium content are shown in Fig. 11, for the 1 wt.% target in Fig. 12.

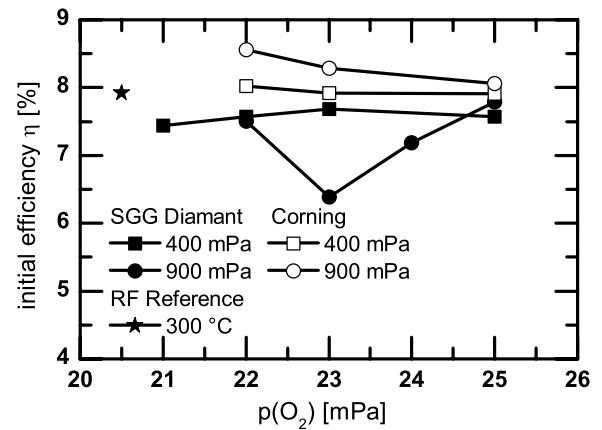


**Fig. 11.** Variation of a-Si:H cell efficiency with oxygen partial pressure and deposition pressure for a AZO film deposited with an aluminium concentration of 2 wt.% in the target. AZO deposition on different glass substrates was carried out at 240 °C.

For the high target concentration all values scatter between 7 and 9%. A slightly better behaviour is observed for the Corning glass substrate which is a lab-quality material. On the Saint Gobain Diamant (SGG) substrate, a low iron content float glass with a thickness of 3.2 mm, the solar cells were only slightly inferior. Nevertheless the process has to be optimised on these type of glass substrates as final production will use them for cost reasons.

From the comparison with an RF sputtered reference sample, deposited in order to monitor the quality of the solar cell process, the results already showed a high potential for the films deposited at 240 °C. Films deposited at lower temperatures were not tested.

For the lower target content a wider screening with solar cells was done. Apart from all samples deposited at 200 °C on SGG Diamant and one on Corning glass, all cells showed initial efficiencies above 7.5%. The reason for the drastically different behaviour of the two substrates is probably the heating process. It is assumed the SGG substrates had a lower temperature when deposition was carried out.

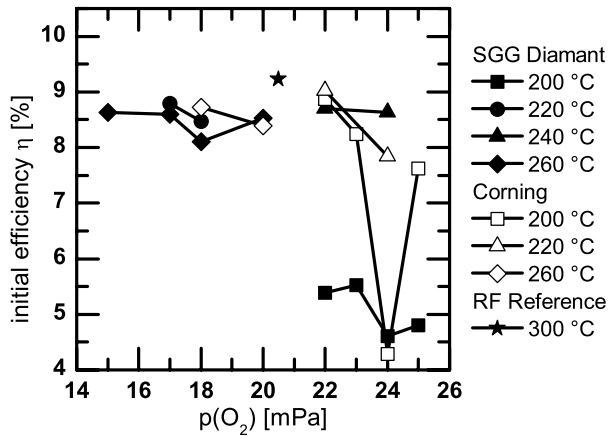


**Fig. 12.** Variation of efficiency with oxygen partial pressure and substrate temperature for a AZO film deposited with a aluminium concentration of 1 wt.% at the target on different glass substrates.

For higher temperatures the cell quality is comparable on both types of substrates and no clear dependence on substrate temperature was observed. The influence of oxygen partial pressure can not be concluded as cell production focussed on a screening of the samples deposited and many AZO films were not tested in solar cells due to high sheet resistances or a bad visual impression after etching. Nevertheless the results indicate that reproducibility was significantly increased and the process is suited as a starting point for further optimisation.

#### 4.4 Multiple pass deposition

In consideration of the positive results obtained by multiple pass depositions at IPV and the problems encountered with the etching behaviour of samples deposited in a single run (Fig. 10), depositions with multiple passes of the carrier in front of the cathode were carried out at IST.

In principle the deposition of a film onto a moving substrate is similar to a stacking of films one would obtain on a static substrate at the positions the carrier passes by [24]. Nevertheless columns grow through the whole film thickness after an interface region on the substrate that can have a thickness of a few monolayers up to 50 or 100 nm. So the interface layer at the substrate influences the bulk properties significantly. In a multiple pass deposition the growth is interrupted in between the different passes. Depending on the coater geometry the growth will initiate once more when the next pass starts. While this may lead to inferior properties, i.e. if the interface region has inferior electrical properties, this deposition technique might be beneficial as shown in Fig. 13. Despite a thorough cleaning procedure there will be particles remaining on the surface. As already

mentioned these particles can act as origins for pinholes impairing etching behaviour (Fig. 10). In multi pass deposition this serious problem can be solved if the pinhole growth is stopped at the interface regions between the films deposited during different passes. Thus defects normally capable of growing through the whole film will be limited to a small part of the film, resulting in an improved and more predictable etching behaviour.

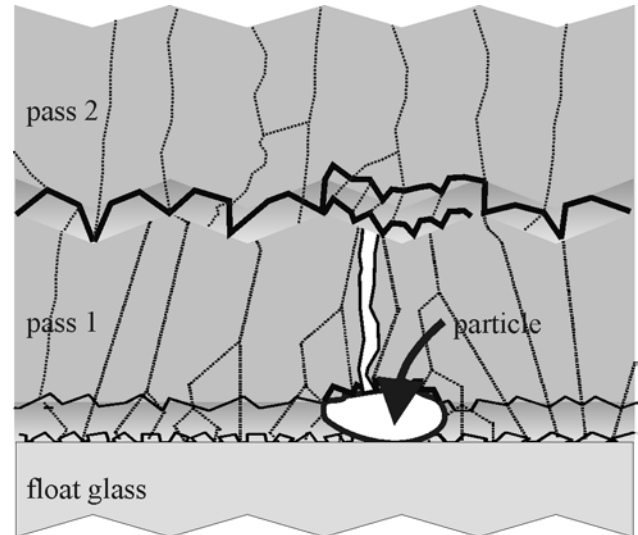


**Fig. 13.** Schematic sketch of the grain growth around a particle by multi pass deposition.

The new deposition series was carried out by passing the substrate four times in front of the target. The same deposition conditions as summarized in table 2 were used with a target concentration of 1 wt.% aluminium. SGG Diamond float glass with a thickness of 3.2 mm and a  $SiO_2$  interface layer deposited after cleaning was used as substrate.

The surface after the removal of 150 nm film thickness by etching was observed by SEM. Fig 14. shows the surface morphology for the low and high pressure region and the typical behaviour which results in smoother surface structures at lower oxygen partial pressure (sample A and B) and very rough surfaces with sharp and comparatively small structures at higher oxygen partial pressure (sample C and D). The images also show the effect of single and multi pass deposition. The single pass deposited sample (sample A and C) shows deeper etching structures than the multi pass deposited sample (sample B and D). This confirms the proposed model and a more predictable etching behaviour with better homogeneity together with a lower defect density caused by the particles is obtained for substrate movement in multiple passes compared to a single pass.

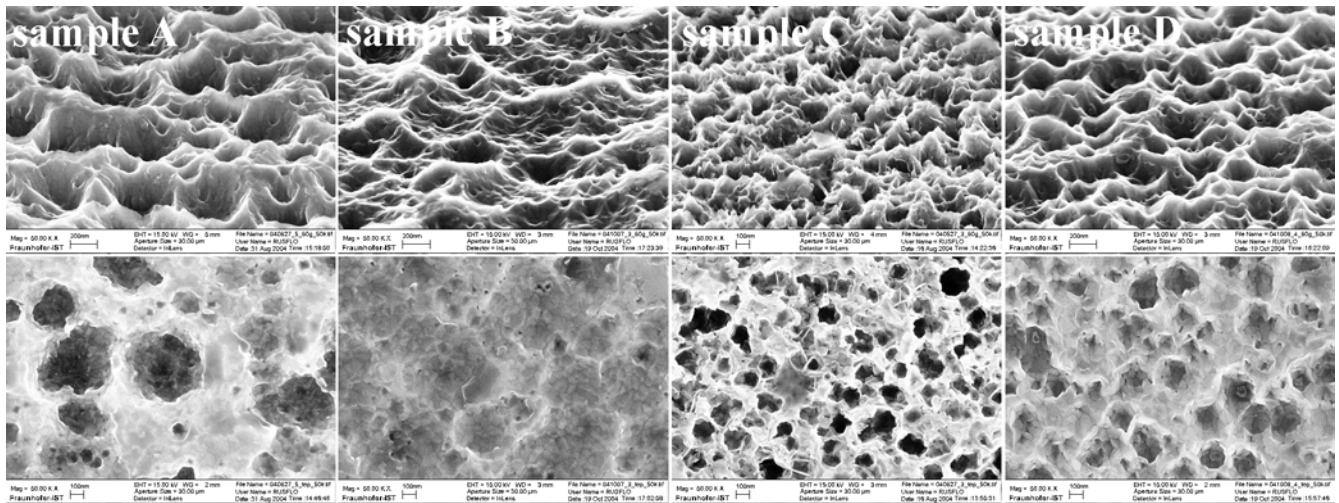


**Fig 14.** SEM images of four etched ZnO:Al films for low (sample A and B) and high oxygen partial pressure (sample C and D) and for single (sample A and C) and multi pass deposition (Sample B and D) after etching in 0.5% HCl removing 150 nm of film thickness. The surface morphology was observed under an angle of 60° (upper row) and in top view (lower row).

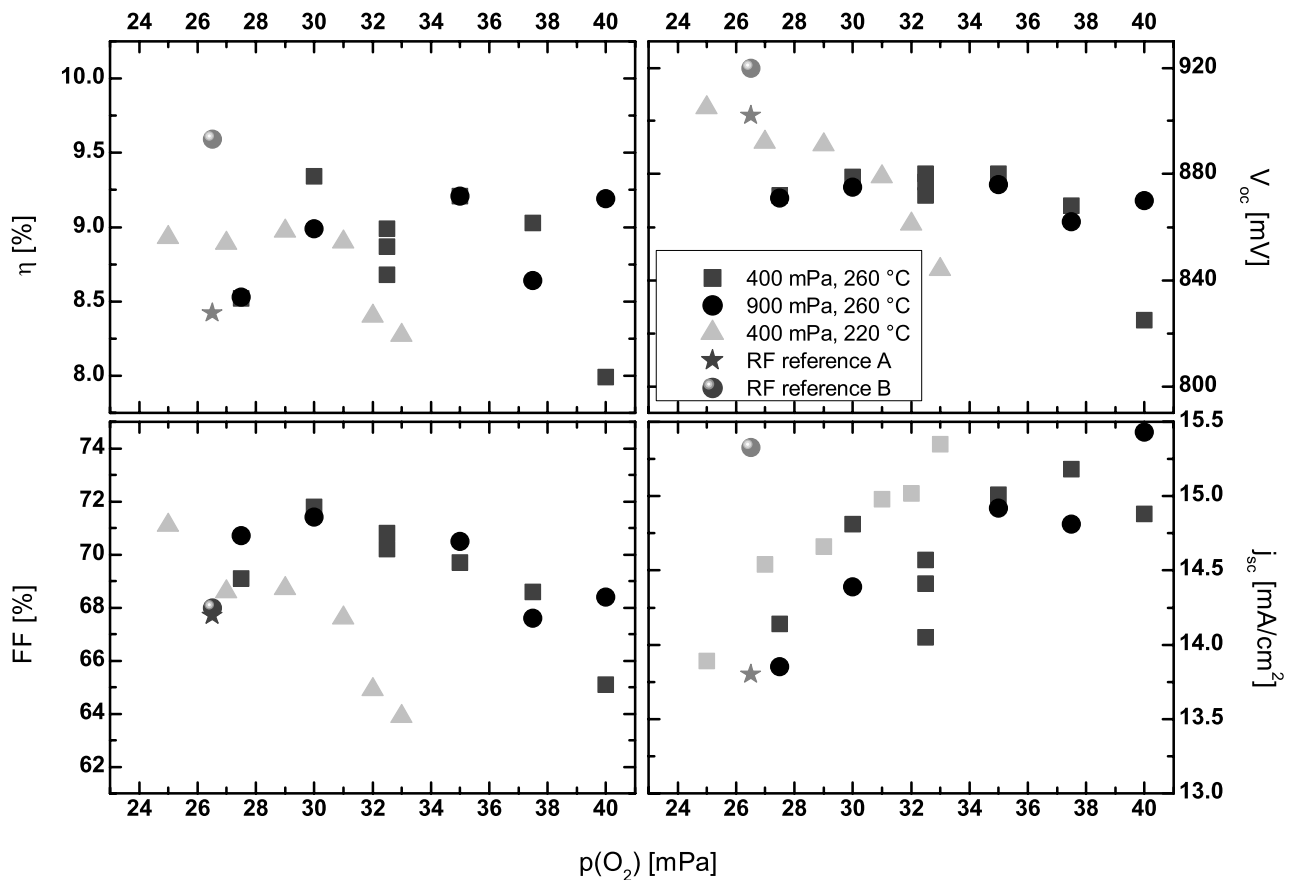


**Fig 15.** Initial efficiency  $\eta$ , open-circuit voltage  $V_{OC}$ , fill factor FF and short-circuit density  $J_{SC}$  of a-Si:H solar cells deposited onto AZO substrates deposited under different conditions with 4 passes in front of the cathodes. Reference A refers to the sample with AZO deposited at 260 °C, reference B refers to sample deposited at 220 °C.

A-Si:H solar cells were deposited onto AZO coated substrates that had been prepared using different oxygen partial pressures, substrate temperatures of 220 and 260 °C and chamber pressures of 400 and 900 mPa. The solar cells were characterised at IPV by illuminated current-voltage (J-V) measurements. It turned out that the introduction of the multi pass AZO deposition led to significant improvements regarding cell efficiency and reproducibility: All initial solar cell efficiencies are near or over 9 % within a wide oxygen partial pressure range (Fig. 15).

An influence of the substrate temperature is revealed since the sample with AZO deposition at 260 °C shows a slightly better performance compared to 220 °C. In spite of an almost constant efficiency with respect to oxygen partial pressure there is considerable variation in open-circuit voltage  $V_{oc}$ , fill factor FF, and short-circuit current density  $j_{sc}$ . The short-circuit density  $j_{sc}$  increases with increasing oxygen partial pressure. This is a clear sign of an improved light trapping with increasing surface roughness. Unfortunately the effect is accompanied by decreasing open-circuit voltage  $V_{oc}$  and fill factor FF for films deposited at high oxygen partial pressures.

As seen in Fig. 6 and Fig. 14 the surface gets rougher after etching with increasing oxygen partial pressure. This also causes a larger surface, increasing the dark current of the p-i-n diode. In consequence the open circuit voltage  $V_{oc}$  will drop. The fill factor will also diminish with increasing oxygen partial pressure due to increasing sheet resistances, especially after etching. This problem can in principle be ruled out by thicker TCO films but only at the cost of longer deposition times and higher optical losses. Moreover, both  $V_{oc}$  and the fill factor FF may suffer from local shunting at spikes. In consequence the broad efficiency maximum is limited by a compromise between achievable current and reachable electrical performance. Future work is dedicated to a fine optimisation of the TCO surface to obtain an optimal light trapping while high FF and  $V_{oc}$  are maintained.

For further evaluation a-Si:H and a-Si:H/ $\mu$ Si:H test mini modules (aperture area 64 cm<sup>2</sup>) with AZO films deposited on commercial SGG substrates were prepared. The initial parameters achieved are shown in table 3.

**Table 3.** Performance of an a-Si:H und an a-Si:H/ $\mu$ c-Si:H mini-module tested on the substrates produced in multi-pass deposition.

	$\eta$ (%)	$V_{oc}$ (V)	$J_{sc}$	FF
a-Si:H	7.4	7.4	12.93	64.3
a-Si:H/ $\mu$ Si:H	9.6	10.4	10.38	67.0

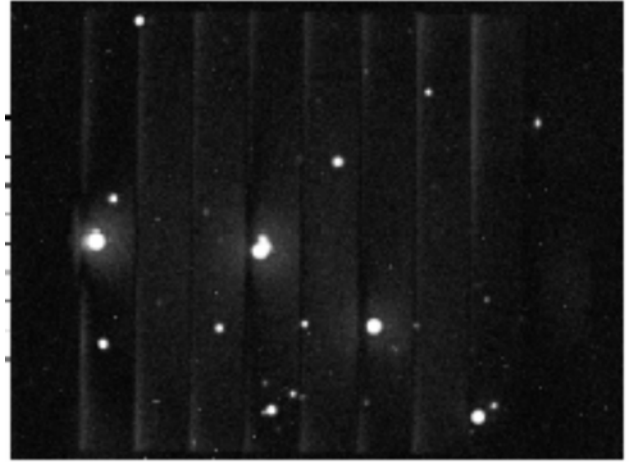


**Fig. 16.** Thermographic measurement of an a-Si:H mini module on 10 x 10 cm<sup>2</sup> substrate size (aperture area 64 cm<sup>2</sup>).

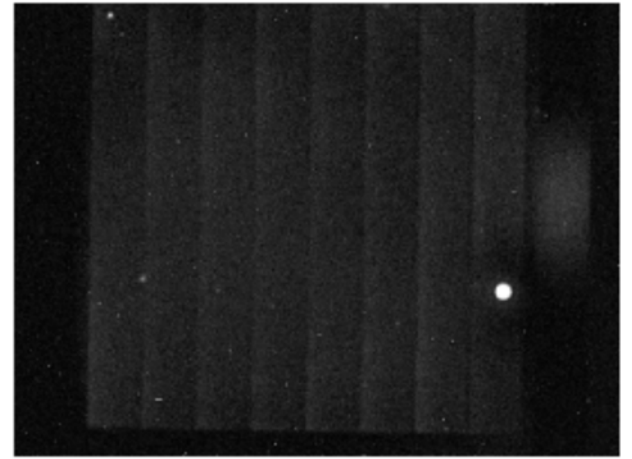


**Fig. 17.** Thermographic measurement of an a-Si:H/ $\mu$ Si:H tandem mini module on 10 x 10 cm<sup>2</sup> substrate size (aperture area 64 cm<sup>2</sup>).

Nevertheless the low fill factors of the a-Si:H modules are caused by local shunts which are indicated by thermography measurements (Fig 16). The module is structured from top to bottom and the white spots show areas of high temperature, usually caused by high current density at shunts. The same problem, only to a lesser extend, can be seen at the a-Si:H/ $\mu$ Si:H tandem mini module for which only one local shunt visualized by thermography measurements is observed (Fig 17). The tandem cells are much less sensible to local shunting due to the thick  $\mu$ c-Si:H i-layer.

The main reason for the shunts is the above mentioned particles leading to pinholes during the the deposition process. The origin of the particles is unclear, with insufficient cleaning only being one of the possible explanations. A second possible contamination source is the cathode itself, as redeposition taking place at the edge of the racetrack can lead to severe flaking with increasing lifetime of the target. Fig. 18 shows a photograph of

the target surface of a TwinMag™ (left) and a CleanMag™ (right) cathode after long term deposition of AZO films without any additional cleaning cycle for both magnetrons.

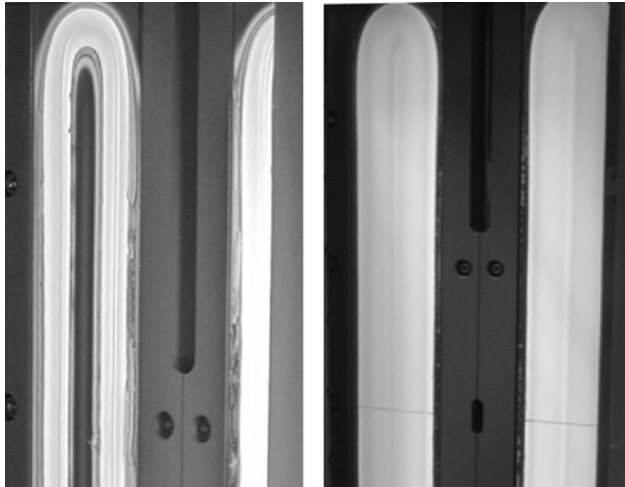


**Fig. 18.** Pictures of the target erosion for a TwinMag™ (left) and a CleanMag™ (right) cathode.

In contrast to the conventional stationary magnets, the CleanMag targets exhibit a sputtered metallic surface over a wide range. No re-deposition zone between the racetracks can be seen. More aspects of the CleanMag technology can be found in [25].

## 5. Conclusions and outlook

It was shown that sputtered ZnO:Al films are a good candidate as front contacts in amorphous silicon solar cells. Using a low-cost reactive sputtering technique from metallic targets the films are attractive from a financial point of view compared to ZnO-based films deposited with alternative techniques or SnO-based TCO layers.

As shown the film properties can be customised by an appropriate choice of deposition conditions and films well suited for amorphous silicon solar cells are obtained. The most important aspects discussed here were substrate cleaning, high temperature deposition and multi-pass deposition.

As far as the substrate cleaning is concerned less problems will arise if a pilot production can be established, in which cleaning can take place directly before coating and where etching and cell deposition can be done without shipping samples between different laboratories. Nevertheless particles can still be an issue for large area modules. Moving magnets to prevent flaking, additionally reducing costs by increased target utilisation, and a better cleaning procedure promise to be successful. Display manufacturers have already shown low contamination processes can be put into practice.

A multi-pass deposition might not be favourable for an in-line process at first sight, but it is likely AZO

deposition will be realised in a coater with multiple deposition stations, so that the substrate will pass three or more coating compartments and thus obtain a multilayer structure.

The last aspect involved is the increased substrate temperature which always raises costs significantly. While 150 °C are normally sufficient to obtain low resistivities and a high optical transmission, the etching behaviour is rather unpredictable and process windows for TCO films for high efficiency solar cells are difficult to establish. Raising the substrate temperature to temperatures above 200 °C improves the situation, with cell results being more predictable and the reactive sputtering process much more stable. A possible hazard is the Zn desorption that can cause serious problems. Up to now neither IST nor IPV have noticed any interference with coater performance by Zn growth on the chamber walls. Nevertheless target utilisation has to be studied closer as this, together with substrate heating, can be one of the major cost aspects in mass production.

## Acknowledgements

The authors would like to thank J. Müller for long time coordination of the research project and many valuable discussions. Fruitful input from our other project partners, namely Applied Films, RWE Schott Solar, Saint Gobain Glas, Sentech Instruments and RWTH Aachen, is gratefully acknowledged. This work was supported by the Federal Ministry for the Environment, Nature Conservation and Nuclear Safety, BMU under contract No. 0329923A.

## References

- [1] M. Schmela, *PHOTON international* 3/2005 (2005), p. 66-82.
- [2] B. Rech, H. Wagner, *Applied Physics A* 69 (1999), p. 155-167.
- [3] O. Vetterl, F. Finger, R. Carius, P. Hapke, L. Houben, O. Kluth, A. Lambertz, A. Mück, B. Rech, H. Wagner, *Solar Energy Materials and Solar Cells* 62 (2000), p. 97-108.
- [4] J. Springer, A. Poruba, M. Vanecek, S. Fay, L. Feitknecht, N. Wyrsh, J. Meier, A. Shah, T. Repmann, O. Kluth, H. Stiebig, B. Rech, *Proceedings 17<sup>th</sup> European Photovoltaic Solar Energy Conference Munich, Germany* (2001), p. 2830.
- [5] B. T. Grundy, E. Hargreaves, K. Franz, *EU Patent* 0 365 239 B1, 28 April 1993.
- [6] O. Kluth, B. Rech, L. Houben, S. Wieder, G. Schöpe, C. Beneking, H. Wagner, A. Löffl, H. W. Schock, *Thin Solid Films* 351 (1999), p. 247-253.

- [7] N. Malkomes, M. Vergöhl, B. Szyszka, J. Vac. Sci. Technol. A 19(2) (2001), p. 414-419.
- [8] B. Szyszka, T.Höing, X. Jiang, A. Bierhals, N. Malkomes, M. Vergöhl, V. Sittinger, U. Bringmann, G. Bräuer, Society of Vacuum Coaters, 44th Annual Technical Conference Proceedings (2001) p. 272-276.
- [9] R. J. Hong, X. Jiang, V. Sittinger, B. Szyszka, T. Höing, G. Bräuer, G. Heide, G. H. Frischat, Journal of Vacuum Science and Technology A 20(3) (2002), p. 900-905.
- [10] B. Szyszka, V. Sittinger, X. Jiang, R.J. Hong, W. Werner, A. Pflug, M. Ruske, A. Lopp, Thin Solid Films 442 (2003), p. 179-183.
- [11] J. Müller, G. Schöpe, O. Kluth, B. Rech, V. Sittinger, B. Szyszka, R. Geyer, P. Lechner, H. Schade, M. Ruske, G. Dittmar, H-P. Bochem, Thin Solid Films 442 (2003), p.158-162.
- [12] J. Müller, G. Schöpe, O. Kluth, B. Rech, B. Szyszka, T. Höing, V. Sittinger, X. Jiang, G. Bräuer, R. Geyer, P. Lechner, H. Schade, M. Ruske, 17th European Photovoltaic Solar Energy Conference, Munich, Germany, October 22-26, 2001.
- [13] J. Müller, G. Schöpe, O. Kluth, B. Rech, M. Ruske, J. Trube, B. Szyszka, X. Jiang, G. Bräuer, Thin Solid Films 392 (2001), p. 327-333.
- [14] A. Lopp, J. Trube, M. Ruske, H. Claus, SID 02 Digest of Technical Papers 33 No. 1, 309-311.
- [15] J. Hüpkes, B. Rech, B. Sehrbrock, O. Kluth, J. Müller, H.-P. Bochem, M. Wuttig, Proceedings 19th European Photovoltaic Solar Energy Conference, Paris, France, Vol. II (2004), p. 1415-1418.
- [16] S. Berg, H.-O. Blom, M. Moradi, C. Nender, T. Larsson, J. Vac. Sci. Technol. A 7(3) (1989), p. 1225-1229.
- [17] A. Pflug, B. Szyszka, V. Sittinger, J. Niemann, Society of Vacuum Coaters, 46th Annual Technical Conference Proceedings (2003) p. 241-247.
- [18] F. Ruske, A. Pflug, V. Sittinger, W. Werner, B. Szyszka, Proceedings of 5th International Conference on Coatings on Glass, Saarbrücken, Germany (2004), p. 125-128.
- [19] J. Müller, G. Schöpe, B. Rech, H. Schade, P. Lechner, R. Geyer, H. Stiebig, W. Reetz, Proceedings of 3rd World Conference on Photovoltaic Energy Conversion (Osaka, 2003), p. 1839-1842
- [20] J. Hüpkes, B. Rech, O. Kluth, T. Repmann, B. Sehrbrock, J. Müller, R. Drese, M. Wuttig, Technical Digest of the 14th International Photovoltaic Science and Engineering Conference 2004, Vol. 1, Bangkok, Thailand, p. 379-380.
- [21] J. Hüpkes, B. Rech, S. Calnan, O. Kluth, U. Zastrow, H. Siekmann, M. Wuttig, Proceedings of 5th International Conference on Coatings on Glass, Saarbrücken, Germany (2004), p. 895-903.
- [22] J. Hüpkes, PhD thesis, RWTH Aachen, handed in for evaluation.
- [23] B. Rech, O. Kluth, T. Repmann, T. Roschek, J. Springer, J. Müller, F. Finger, H. Stiebig, H. Wagner, Solar Energy Materials and Solar Cells 74 (2002), p. 439-447.
- [24] R. J. Hong, X. Jiang, B. Szyszka, V. Sittinger, S. H. Xu, W. Werner, G. Heide, Journal of Crystal Growth 253 (2003), p. 117-28.
- [25] V. Sittinger, B. Szyszka, R.J. Hong, W. Werner, M. Ruske, A. Lopp, Proceedings of 3rd World Conference on Photovoltaic Energy Conversion (Osaka, 2003), p. 503-506.